Journal of Sustainable Construction Materials and Technologies
Web page info: https://jscmt.yildiz.edu.tr
DOI: 10.47481/jscmt.1555168

JSCMT
Journal of Sustainable Construction Materials and Technologies

Research Article

High temperature performance of geopolymer: Contribution of boron tincal waste

Zinnur ÇELİK[1], Emrah TURAN*[2], Meral OLTULU[2]

[1]*Atatürk University, Pasinler Vocational School, Erzurum, Türkiye*
[2]*Department of Civil Engineering, Atatürk University Faculty of Engineering, Erzurum, Türkiye*

ARTICLE INFO

Article history
Received: 19 July 2024
Revised: 31 August 2024
Accepted: 01 September 2024

Key words:
Boron, geopolymer, high temperature, tincal waste, strength

ABSTRACT

The world's largest boron deposits are in Türkiye, Russia, and the U.S.A. Türkiye holds about 73% of the world's reserves of oil. The tincal mineral accounts for approximately 25.3% of Türkiye's boron reserves. Annually, around 900,000 tons of boron-derived waste are produced to obtain 1 million tons of borax pentahydrate from the tincal mine. This waste is stored in pools, causing considerable environmental issues. This study investigates the potential use of tincal waste, an environmental problem, in cement and concrete applications. Tincal waste (T.W.) was utilized to produce geopolymer mortar. Geopolymer samples were created by replacing ground blast furnace slag (G.B.F.S.) with 10%, 20%, 30%, and 40% tincal waste (T.W.) by weight. The mixture samples were cured at room temperature and 60 °C. After curing, the samples were exposed to high temperatures of 200 °C, 400 °C, and 600 °C. The samples' unit weight, compressive strength, ultrasonic pulse velocity (U.P.V.), and mass loss values were measured. A mathematical model was also developed to describe the relationship between compressive strength and U.P.V. before and after high temperatures. The samples underwent Fourier Transform Infrared Spectroscopy (FTIR) microstructural analysis. The results showed that using up to 20% T.W. enhanced the properties of the samples before and after high-temperature exposure. A strong correlation was found between compressive strength and U.P.V. These findings suggest that T.W. has potential as a novel material for use in geopolymer technology.

Cite this article as: Çelik, Z., Turan, E., & Oltulu, M. (2024). High temperature performance of geopolymer: Contribution of boron tincal waste. *J Sustain Const Mater Technol*, 9(3), 255–267.

1. INTRODUCTION

Global warming and climate change are recognized worldwide as significant environmental problems of our time [1]. CO_2 emissions are among the most important reasons for this situation. Literature studies report that an essential part of the CO_2 emission occurs during the production phase of O.P.C. [2–4]. It has been reported that producing O.P.C., the primary material for concrete and mortar production, contributes to approximately 5–7% of CO_2 emissions [5]. For decades, researchers have made efforts to reduce the CO_2 load on the planet by producing environmentally responsible concrete, using additional supplementary materials in concrete production [6]. However, supplementary cement materials can partially replace O.P.C., usually 20–30% by weight, due to their adverse effects on concrete workability and early age strength [7].

Geopolymer composites were first named by Davidovits in 1978. The primary material of these three-dimensional amorphous products is aluminosilicates [8, 9]. Geopolymeric cement is called green material because it reduces CO_2 emissions by about 6 times compared to O.P.C., which provides

*Corresponding author.
*E-mail address: emrah.turan@atauni.edu.tr

large energy consumption and carbon dioxide emissions in its production [10]. In addition, geopolymers are an essential part of inorganic polymeric materials with their superior mechanical and thermal properties, low permeability, prominent high-temperature resistance, excellent chemical corrosion resistance, and low density [11–14]. For these reasons, geopolymers in recent years offer an excellent opportunity to replace O.P.C. as cementitious binder material [15]. Recently, geopolymers have been used in ceramics exposed to high temperatures, in coatings, binders, and adhesives for heat-resistant building materials, and as cementing components of concrete and mortar [16]. The most common geopolymers used nowadays are obtained by activating alumino-silicate materials such as fly ash (F.A.), metakaolin, and granulated blast furnace slag (G.B.F.S.) using alkalis such as sodium hydroxide (NaOH), potassium hydroxide (K.O.H.) and sodium silicate (Na_2SiO_3) [17]. The development of mechanical performance in geopolymers depends on the formation of three-dimensional networks consisting of Si-O-Al and Si-O-Si units and the obtained calcium aluminate silicate hydrate (C-A-S-H) and sodium aluminate silicate hydrate (N-A-S-H) gels which depends on the binder composition, curing temperature, activator type and concentration [18–20]. In alkali-aluminosilicate (A.A.S.), calcium-bearing C-(A)-S-H gels predominate with N-A-S-H gels [11].

OPC-based concrete and mortars have low thermal conductivity and are known as non-combustible building materials [21]. Although concrete produced with O.P.C. has significant resistance to high temperatures, $Ca(OH)_2$ decomposes at approximately 400 °C. This phenomenon causes substantial decreases in the strength of OPC-based concrete at temperatures above 400 °C [22, 23]. Geopolymers are considered to have good high-temperature resistance due to their ceramic-like properties [24]. Moreover, the different nature of the hydration products formed in O.P.C. and A.A.S. is the reason for the significant difference in the elevated temperature resistance of geopolymer and regular concrete [25–27]. Guerrieri et al. [28] investigated the residual compressive strength of A.A.S. and O.P.C. paste after being subjected to high temperatures. The study indicates that the residual strength of A.A.S. exposed to 600 °C is similar to O.P.C. Contrary to this study, Türker et al. [29] reported in their research that A.A.S. exposed to 600 °C lost more strength than the O.P.C. specimen. Pan et al. [27] observed the post-high temperature strength values of alkaline activated materials containing G.B.F.S. and Class F F.A. An increase in strength was observed in FA-based samples after 600 °C.

On the contrary, significant decreases in strength occurred in GBFS-based samples at 300 °C compared to O.P.C. binder-based samples. These strength differences reveal substantial differences in the bonding structures of different binder materials at high temperatures. The better behavior of F.A. after high temperature compared to G.B.F.S. was due to the binding phase, N-A-S-H. In recent years, high-temperature performances have been investigated by adding materials such as red mud [30], ferrochrome slag [31, 32], rice husk ash [33] to F.A. and G.B.F.S. based mixtures, as well as the combined use of F.A. and G.B.F.S. binders.

Approximately 73% of the world's stock on reserves is in Türkiye. Türkiye's most important boron ores are tincal, ulexite, and colemanite. The most essential components of boron compounds are boron oxide (B_2O_3) and boric acid (H_2BO_3). These components are called colemanite when bound with calcium, ulexite when bound with calcium-sodium, and tincal when present with sodium [34]. 25.3% of the boron reserve in Türkiye is tincal ore and is located in the Eskişehir Kırka region. To obtain 1 million tons of borax pentahydrate ($Na_2O.\ 2B_2O_3.\ 5H_2O$) from the Tinkal mine, approximately 900000 tons of solid boron derivative waste is generated annually. These wastes are stored in pools and cause significant environmental problems [35–38]. Tinkal waste (T.W.) has been used in many fields, such as ceramics, insulation, and construction, since the 20th century. The use of tincal ore waste as an additional supplementary material in ordinary cement is available in the literature. Kula et al. [39] investigated the usability of T.W., C.B.A., and F.A. as additional cement materials in concrete. Abali et al. [35] studied using tincal waste as a supplementary cement material. As a result, it was stated that as the tincal waste rate increased, the 2-day compressive strength decreased, but at the end of 28 days, the strength approached the reference sample. Boncukcuoğlu et al. [40] used the sieve wastes obtained during borax production from tincal as an additive in the production of O.P.C. They investigated the mechanical properties of the doped O.P.C. Within the scope of the research. It was stated that using 25% by weight of sieve waste as cement additive material would be appropriate.

This study focuses on using tincal ore waste in GBFS-based geopolymer mortars. For this purpose, compressive strength and ultrasonic pulse velocity (U.P.V.) tests were conducted on the 3rd, 7th, and 28th days on geopolymer mortars obtained by replacing G.B.F.S. with tincal waste at rates of 10%, 20%, 30%, and 40%. The prepared mortar samples were either kept at ambient conditions or cured in an oven at 60°C for 24 hours and then kept at ambient conditions until the test day. The produced specimens were subjected to temperatures of 200, 400, and 600°C, and mass loss, compressive strength, and U.P.V. values were investigated. Additionally, a mathematical model was created between compressive strength and U.P.V. before and after high temperature, and the microstructure of the samples was analyzed using FTIR.

1. MATERIALS AND METHODS

1.2. Materials

Within the scope of this research, G.B.F.S. and F.A. were used as binder materials in the reference mixture. G.B.F.S. material was supplied from the Ereğli Iron and Steel Factory, and F.A. material was provided from Çatalağzı power plant. The specific gravity of F.A. and G.B.F.S. are 2.33 and 2.86, and the specific surface area is 2475 cm^2/g and 3824 cm^2/g, respectively. Since the total $SiO_2 + Al_2O_3 + Fe_2O_3$ in the F class F.A. chemical composition is 87.36% and the amount of CaO is 2.44%, it complies with ASTM C 618 [36]. SiO_2/Al_2O_3 by mass of F.A. and G.B.F.S. are 2.91 and

Table 1. Chemical compositions of G.B.F.S., F.A., and T.W.

Oxide (%)	SiO_2	Al_2O_3	Fe_2O_3	CaO	MgO	Na_2O	SO_3	B_2O_3	LOI
GBFS	33.60	11.40	1.10	41.20	6.10	0.40	2.10	–	1.05
FA	60.61	20.81	7.36	2.44	1.64	0.56	0.51	–	2.71
TW	14.12	2.03	0.76	15.87	22.19	8.12	0.53	9.83	23.26

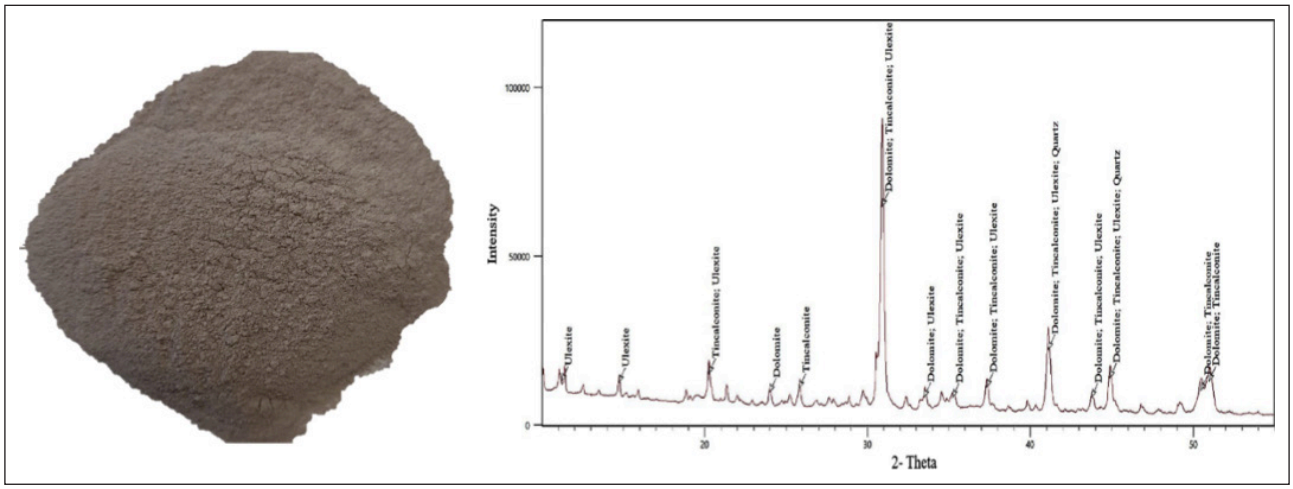

Figure 1. Image and XRD pattern of tincal waste [36].

2.95, respectively. Additionally, tincal waste (T.W.) used in this study was obtained from the Etibank Borax Plant (Kirka, Eskisehir). The specific gravity of tincal waste is 2.48, and the B.E.T. surface area is 65000 cm^2/g. The chemical properties of G.B.F.S., F.A., and T.W. are given in Table 1. According to XRF results (Table 1), the most dominant compounds in the tincal waste sample are magnesium oxide, quartz, and calcium oxide.

The XRD spectrum of tincal waste is shown in Figure 1. The most dominant phases observed in the XRD pattern are dolomite, tincal, quartz, and ulexite.

River sand with the largest grain size of 4 mm and a specific gravity of 2.70 was used to prepare geopolymer mortar samples. The study used sodium hydroxide (NaOH) and sodium silicate (Na_2SiO_3) solution as alkaline activators. The silicate modulus in sodium silicate was equal to 3.18. NaOH solution with a concentration of 12 M, prepared 24 hours in advance, was used to prepare the mixtures. The chemical properties of alkaline activators are given in Table 2.

Table 2. Chemical properties of Na_2SiO_3 and NaOH

Properties	Sodium silicate (Na_2SiO_3)	Sodium hydroxide (NaOH)
Density (g/cm^3)	1.38	2.13
Molecular weight (g/mol)	122.1	40
Color	White	White
pH		13–14
Na_2O (%)	8.9	
SiO_2 (%)	28.3	
H_2O (%)	64.3	

2.2. Mixture Proportions and Test Methods

The mixing ratios of geopolymer mortar samples are given in Table 3. The sand: binder: alkali solution ratio in geopolymer mortar mixtures was 3:1:0.50. Na_2SiO_3 / NaOH solution ratio 2. G.B.F.S. replaced T.W. by 0%, 10%, 20%, 30% and 40%. G.B.F.S., T.W., and F.A. were mixed for 90 s during the mortar preparation. After the first mixing process, 12 M NaOH solution and Na_2SiO_3 prepared the day before were added to the mixture and mixed for another 3 min. Finally, river sand was added to the mixture, and after mixing for another 4 minutes, the mortar was prepared. The prepared mortar mixtures were filled into 50 x 50 x 50 cube samples, and vibration was applied. A group of cube samples prepared by filling molds was kept in ambient cure until the test day. The other group was cured in a laboratory oven at 60 °C for 24 hours. After the specimens were cured for 24 hours, they were stored at room conditions until the test day. The compressive strengths of the samples in both cure groups on the 3rd, 7th, and 28th days were determined according to ASTM C109 [38]. Additionally, U.P.V. and dry unit weights on the 28th day were determined. All mixture series were exposed to 200, 400, and 600 °C temperatures in the oven with a temperature regime of 5 °C/min for 28 days [41]. Compressive strength, U.P.V. value, and mass losses of the mixtures after high temperature were determined.

3. RESULTS AND DISCUSSION

3.1. Dry Unit Weight

The effects of T.W., ambient curing (20 °C), and heat curing (60 °C) for 28 days on the unit weight of the geopolymer mortar specimen are presented in Figure 2. The

Table 3. Mixing ratios of geopolymer mortars

Specimen codes	G.B.F.S. (g)	T.W. (g)	F.A. (g)	Sand (g)	Na_2SiO_3 solution (g)	NaOH solution (g)
Control	405		45	1350	150	75
TW-10	360	45	45	1350	150	75
TW-20	315	90	45	1350	150	75
TW-30	270	135	45	1350	150	75
TW-4	225	180	45	1350	150	75

unit weights of the samples kept in the ambient cure ranged from 2120 to 2223 kg/m^3. The lowest unit weight value was obtained from the TW-40 series, and the highest was obtained from the TW-10 series. Substitution of 10% and 20% T.W. increased the unit weights by 2.82% and 1.94%, respectively, compared to the reference sample. Unit weights were decreased as the T.W. ratio increased to 30% and 40%.

The unit weights of the samples cured at 60 °C ranged between 2138 and 2250 kg/m^3. Similar to the samples in ambient cure, the highest unit weight was calculated in the TW-10 series with 2250 kg/m^3. This value was 2.74% higher than the control sample. The unit weight of the TW-40 mixture was approximately 2.34% less than the control sample. The values obtained from heat curing were higher than those obtained in the ambient cure. This can be attributed to heat curing accelerating the hydration reaction and higher bulk density. In the control and TW-10 series, 1.30% and 1.21% increase in unit weights was calculated as the curing rate increased by 60 °C compared to the ambient cure.

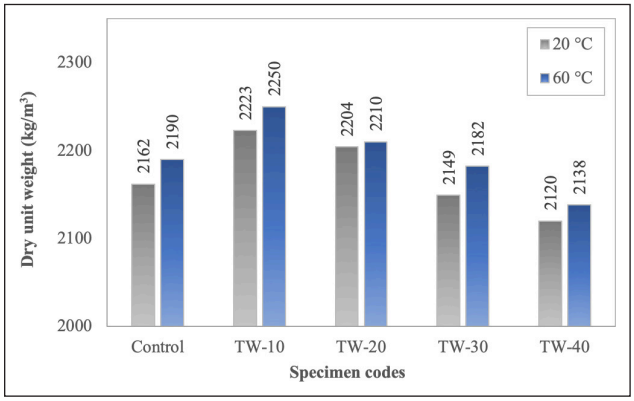

Figure 2. Dry unit weight of geopolymer mortars.

3.2. Compressive Strengths

3.2.1. Curing at Ambient Temperature

The compressive strength test results of the mixtures at ambient temperature conditions on 3, 7, and 28 days are given in Figure 3. The 3 days compressive strength of the mixture samples varies between 16.09 MPa and 30.75 MPa. The highest 3-day compressive strength was obtained from the TW-10 series with 30.75 MPa. As a result of increasing curing time, compressive strength improved significantly. The highest 7-day compressive strength was obtained in the mortar mixture using 10% T.W. An improvement of 30.25% and 7.65%, respectively, was detected in the compressive strengths of mixtures using 10% and 20% T.W. compared to the control specimen.

The strength results of the mixtures on the 28th day were also compatible with the 3 and 7-day strength values. The strength results on the 28th day showed that the mixtures varied between 30.30 MPa and 60.70 MPa. The highest compressive strength value was detected in the TW-10 series. According to the reference mixture, substituting 10% T.W. increased the strength by 28.60%. Although mixtures containing 30% and 40% T.W. showed a particular strength improvement, their performance was lower than the control sample. Compared to the control mixture, a decrease of 15.67% and 35.8% was achieved in the compressive strengths obtained from the TW-30 and TW-40 series. As a result, 10% and 20% T.W. substitution increased the series' strength at all ages. This increase in compressive strength can be attributed to the development of geopolymerization and the production of additional sodium aluminosilicate hydrate (NASH) gel due to the Na_2O contained in T.W. Additionally, unlike G.B.F.S., which is high in calcium, T.W. contains high amounts of magnesium. This is one of the most critical factors causing the improvement in compressive strength, attributable to the high magnesium content, which behaves similarly to calcium and forms a new hydrate gel called a hydrotalcite-like phase or magnesium-containing silicate hydrates M-S-H and C-M-S-H [42, 43]. Bouaissi et al. [42] produced geopolymer mortars using different substitutes of high magnesium nickel slag (H.M.N.S.), F.A. and G.B.F.S. The research reported that the 14-day compressive strength of mixtures containing 10% H.M.N.S. increased by 29% compared to the reference series. Zhang et al. [43] stated that the strength of geopolymer mortars is 20% and 40% H.M.N.S. Replacement was higher

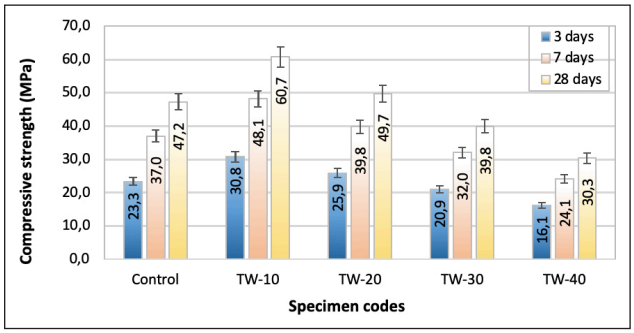

Figure 3. Compressive strength of specimens cured at ambient temperature.

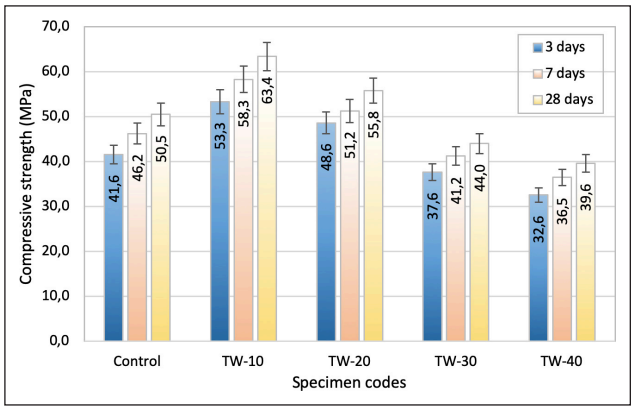

Figure 4. Compressive strength of specimens heat curing at 60° C.

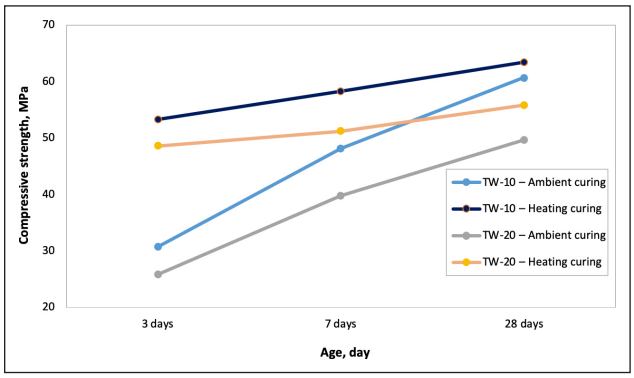

Figure 5. Effect of room temperature and heat curing on TW-10 and TW-20 series.

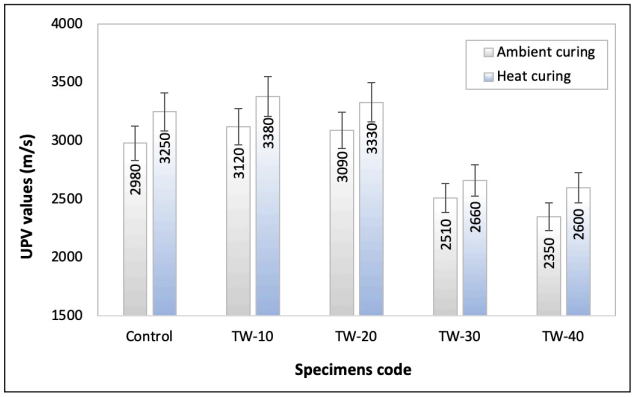

Figure 6. Ultrasonic pulse velocity values of geopolymer mortars.

than the mixture containing 100% FA. Ben Haha et al. [44] stated that slag containing high amounts of MgO increases the formation of a hydrotalcite-like phase due to hydration and reduces Al uptake by C-S-H. Uysal et al. [45] investigated using colemanite, another type of boron mineral, to produce geopolymer mortar. As a result of the study, it was determined that the use of 10% colemanite waste increased the compressive strength by 2.02%, while its substitution at 20% decreased the strength by 20.74%.

3.2.2 Heat Curing at 60 °C

Compressive strength data of specimens heat cured at 60° C are presented in Figure 4. 3 days of compressive strength of mortars ranged between 32.56 and 53.32 MPa. The highest strength value was obtained from the TW-10 series, with an increase of approximately 28.32% compared to the control specimen. Curing at 60°C remarkably affected the strength of mortars containing G.B.F.S. and T.W at an early age. The 3-day compressive strength of specimens cured at high temperatures was higher, in the range of approximately 73%–102%, compared to specimens cured at ambient temperature. Görhan et al. [46] stated that high-temperature curing did not have a remarkable effect on the physical properties of geopolymer mortars but caused an increase in compressive strength. There was an increase in strength as the cure period increased to 7 days. While the highest compressive strength was calculated from the TW-10, the lowest strength value was observed in the TW-40 series. Using 10% and 20%, T.W. improved the compressive strength by about 26% and 10.8%, compared to the control mixture.

The 28-day strength of mixtures cured at 60 °C gave similar results to the three and 7-day strengths. The highest 28-day strength result was observed in the TW-10 series, with 63.40 MPa. This value was 25% higher than the control specimen. It was observed that 30% and 40% T.W. substitution reduced the compressive strength by 12.87% and 21.58%, compared to the reference mixture. According to the results of these studies, it can be reported that the 28-day strength of specimens kept at room temperature approaches the results of samples cured at 60 °C (Fig. 5). This result is consistent with the results of previous studies in the literature [47]. It was determined that the compressive strength of heat-cured specimens after 28 days varied between approximately 4% and 30% compared to specimens cured at ambient temperature.

3.3. Ultrasonic Pulse Velocity (U.P.V.)

Ultrasonic pulse velocity test (U.P.V.) is a non-destructive testing method to examine the homogeneity of the geopolymer mortar matrix and the presence of any defects. U.P.V. results of geopolymer mortars at 28 days are given in Figure 6. U.P.V. values of 10% and 20% T.W. mixture mortars increased compared to the control sample in ambient and Heat cured. The U.P.V. value of the ambient cured TW-10 series was 4.69% higher than the control mixture. This value is determined as 4% in the heat-cured TW-10 series. As the T.W. ratio in the mixtures increased, U.P.V. values tended to decrease, similar to the compressive strength results. The velocity values of the 30% T.W. substituted mortar series after curing with the environment, and Heat decreased by approximately 15% and 18% compared to the reference specimen.

3.4. FT-IR Analysis

Fourier transform infrared spectroscopy (FTIR) is an effective method to detect the presence of chemical bonds and products formed during geopolymerization. FTIR spectra of geopolymer mortars are given in Figure 7. The broad band centered at 3360 cm^{-1} arises from the overlap of symmetric

Table 4. Changes of geopolymer mortars subjected to ambient cured after elevated temperature

Specimen code	Change in compressive strength, %			Change in U.P.V., %		
	200 °C	400 °C	600 °C	200 °C	400 °C	600 °C
Control	-3.60	-22.03	-49.36	-12.75	-29.53	-62.42
TW-10	-2.14	-17.13	-43.00	-6.41	-27.56	-59.62
TW-20	-6.44	-12.27	-47.69	-9.39	-28.16	-61.17
TW-30	-13.07	-27.39	-43.47	-12.35	-23.51	-60.96
TW-40	-24.75	-47.85	-68.32	-14.89	-31.91	-67.66

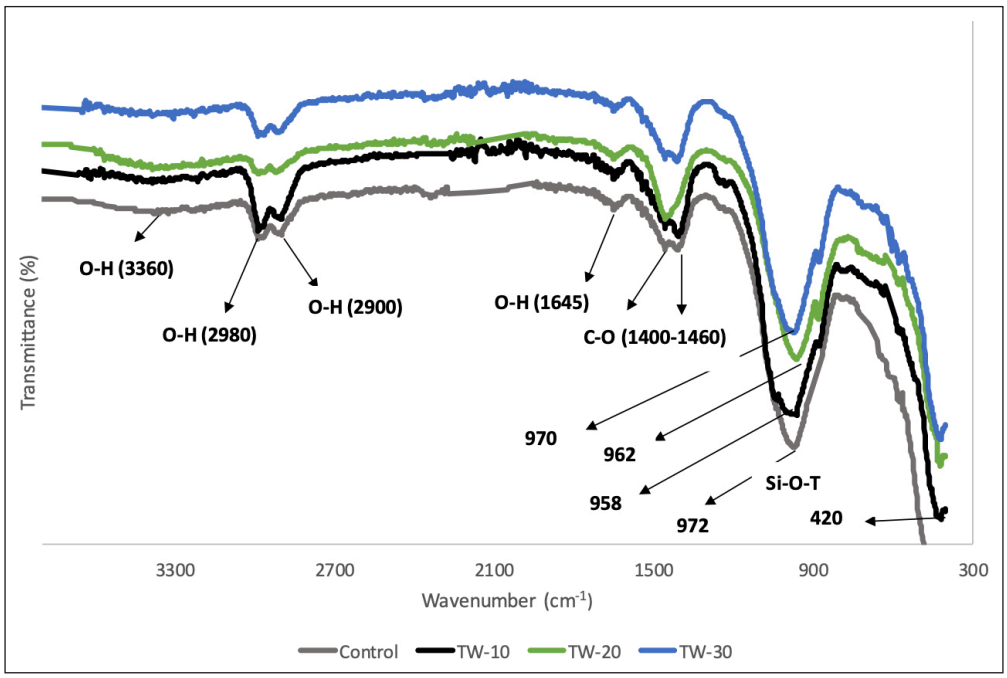

Figure 7. FTIR spectra of geopolymer mortars.

and asymmetric stretching of the O-H bending of absorbed water in the bands at 3300–3600 cm^{-1} [42, 43]. The peak of the wave number at 2980 cm^{-1} indicates the stretching vibration of the hydrogen-bonded O-H group, and the peak at 2900 cm^{-1} indicates the bending vibration of the O-H group [44, 45]. O-H bending vibrations associated with hydrated products are represented by the band determined at approximately 1645 cm^{-1}. These O-H groups refer to structural and entrapped water in sodium aluminosilicate (N-A-S-H) gels [44, 48]. The peaks at 1460 and 1400 cm^{-1}, which characterize the stretching vibration of the C-O bond, are associated with sodium bicarbonate (Na_2CO_3) [47, 49, 50].

Approximately 958–972 cm^{-1} bands are an essential point of the geopolymer, showing the asymmetric stretching vibration of the Si-O-T (T=Al or Si) bond. With the addition of T.W. to geopolymer mortars, the reference sample's 972 cm^{-1} Si-O-T stretching vibration was determined as 958 cm^{-1} and 962 cm^{-1} from the TW-10 and TW-20 series, respectively. Shifts in this band cause geopolymerization acceleration, structure strengthening, and strength improvement [48]. This shift in Si-O-T asymmetric vibration can be attributed to incorporating Al and Mg into the content of silicate hydrate gels [43].

As a result of the use of materials containing high amounts of MgO in geopolymer production, it has been proven in previous studies that Mg^{2+}, such as Al^{3+}, can replace Si^{4+} and the formation of gels such as Na-Al (Mg)-Si-O-H [43, 51]. Moreover, the formation of a broad band with a strong shoulder of approximately 860 cm^{-1} with the addition of T.W., except for the reference sample, indicates the sizeable stretching area of the O-Si bond resulting from the addition of Mg to the silicate network [43, 52]. Another indication of Mg presence can be associated with the band vibration at approximately 420 cm^{-1} [53]. Mg^{++} content in the geopolymeric chain contributes to the matrix's chemical stability or interatomic bonding by forming different connections, such as Si-O-Mg, Si-O-Al, Ca-O-Si, and Si-O-Si [42].

3.5. Properties After Elevated Temperature Exposure

The compressive strength results of geopolymer mortars subjected to ambient cured after high temperature are shown in Figure 8, and the compressive strength and U.P.V. changes are given in Table 4.

The compressive strengths of control, TW-10, and TW-20 mixtures cured in the ambient did not show a remarkable decrease at 200 °C. As a result of exposure of the reference

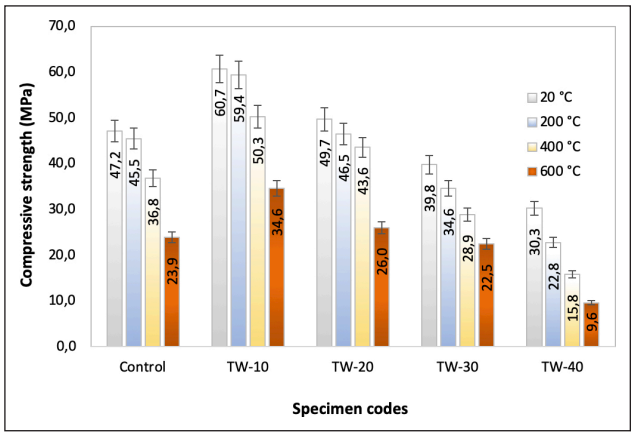

Figure 8. Compressive strengths of mortar samples in ambient cured after high temperature.

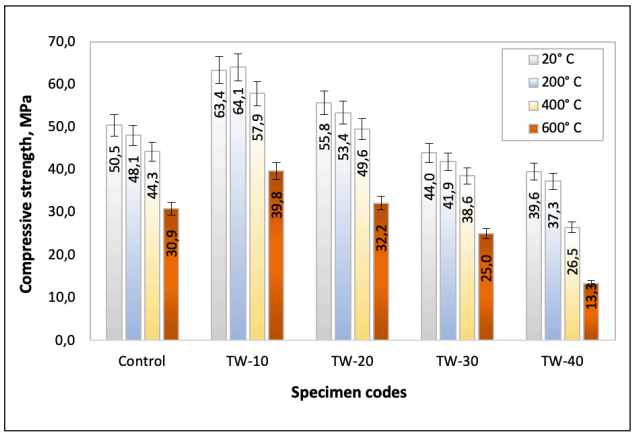

Figure 9. Compressive strength of heat-cured mortar samples after high temperature.

specimen kept in ambient cured to 200 °C, there was a 3.60% decrease in compressive strength. The lowest reduction of compressive strength at 200 °C was obtained from the TW-10 series with 2.14%. As the T.W. ratio used in the mixtures increased to 30% and 40%, a decrease of 13.07% and 24.75% in strength was observed, respectively. The compressive strength of geopolymer mortar specimens subjected to ambient curing tended to decrease as the temperature increased. In their study, Zhang et al. [54] reported that geopolymer mortars' flexural and compressive strengths increased at 100 °C and decreased with increased temperatures.

As the temperature increased to 400 °C, the decreases in strength became more evident. The compressive strength of the control sample decreased by 22.03%. The reduction in strength of mixtures using 10% and 20% T.W. was determined as 17.13% and 12.27%, respectively. Although the decreases in the strength of TW-10 and TW-20 were lower compared to the reference sample, the strength losses increased with the increase in the T.W. ratio. The reduction in strength of geopolymer mortar samples exposed to 600 °C ranged from 43.00% to 68.32%. The decrease in strength of the control sample was determined as 49.36%. Substitution of 40% T.W. reduced the strength at 600 °C by 68.32% compared to the initial strength. This is because when geopolymer mortars were exposed to high temperatures, the free water in the matrix evaporated, and the strength decreased due to dehydration [55–58]. Evaporation in the matrix increased with the increase in temperature, causing internal pressure. After the internal pressure reached a specific limit, the resistance of the composite to thermal effects decreased, causing cracks on the surfaces.

Moreover, high temperatures created thermal mismatches by creating microcracks at the interface transition area between aggregate and paste [58, 59]. However, the decrease in the strength of the mixtures using 10%, 20%, and 30% T.W. at 600 °C was less than the reference specimen. The least strength loss was reported in the TW-10 series, at 43%. Geopolymers are believed to have excellent bonding ability due to the formation of a three-dimensional N-A-S-H type gel, which is a network [Q^4(Al)] composed of SiO_4 and AlO_4 tetrahedral, which form a bonding structure between each other with shared O atoms. This structure gives geopolymer mortars significant high-temperature resistance [27, 60]. The T.W. used in this study contains Na_2O. This component may have formed an additional N-A-S-H structure in the geopolymer mortar structure. This may be one of the reasons why the high-temperature resistance of mixtures containing T.W. loses less strength compared to the reference sample.

Additionally, Lee et al. [61] investigated the effect of G.B.F.S. addition on the structure of FA-based geopolymers. They reported that the C-(A)-S-H structure formed in mixtures containing G.B.F.S. is vulnerable to thermal structure degradation. Contrary to this situation, the increase in the high-temperature resistance of the mixtures in this study can be attributed to the addition of T.W. producing the N-A(M)-S-H gel phase by containing high amounts of Mg. Yang et al. [62] stated that F.A. mixtures with nickel slag containing high amounts of magnesium produced N-A(M)-S-H, which improved the mixtures' thermal stability. However, they reported that the mechanism causing this situation is still unclear.

The U.P.V. results of the mortars are presented in Table 4. The reduction in U.P.V. values of the specimens was between 6.41% and 14.89% at 200 °C. The lowest loss in U.P.V. value was obtained in the TW-10 series, similar to the results in compressive strength. Additionally, using 10% and 20%, T.W. caused less decrease in U.P.V. values compared to the control sample. The reduction in U.P.V. results continued as the temperature increased to 400 °C. While the reduction of the reference sample was 29.53%, the decrease in the TW-10 and TW-20 series was calculated as 27.56% and 28.16%. As the temperature increased to 600 °C, a significant decrease was observed in the U.P.V. values of geopolymer mortars. 10% and 20% T.W. substitution reduced U.P.V. values by 59.62% and 61.17%. This rate was measured as 62.42% in the reference sample. Although there is a proportional difference between compressive strength and U.P.V. results, they are similar in trend.

The compressive strength results of geopolymer mortars subjected to Heat cured after high temperature are shown in Figure 9, and the compressive strength and U.P.V. changes

Table 5. Changes of geopolymer mortars subjected to Heat cured after elevated temperature

Specimen code	Change in compressive strength, %			Change in U.P.V., %		
	200 °C	400 °C	600 °C	200 °C	400 °C	600 °C
Control	-4.75	-12.28	-38.81	-11.08	-27.38	-59.38
TW-10	1.10	-8.68	-37.22	-5.33	-25.44	-57.10
TW-20	-4.30	-11.11	-42.29	-8.11	-24.92	-57.06
TW-30	-4.77	-12.27	-43.18	-8.27	-21.80	-49.62
TW-40	-5.81	-33.08	-66.41	-9.23	-26.92	-63.08

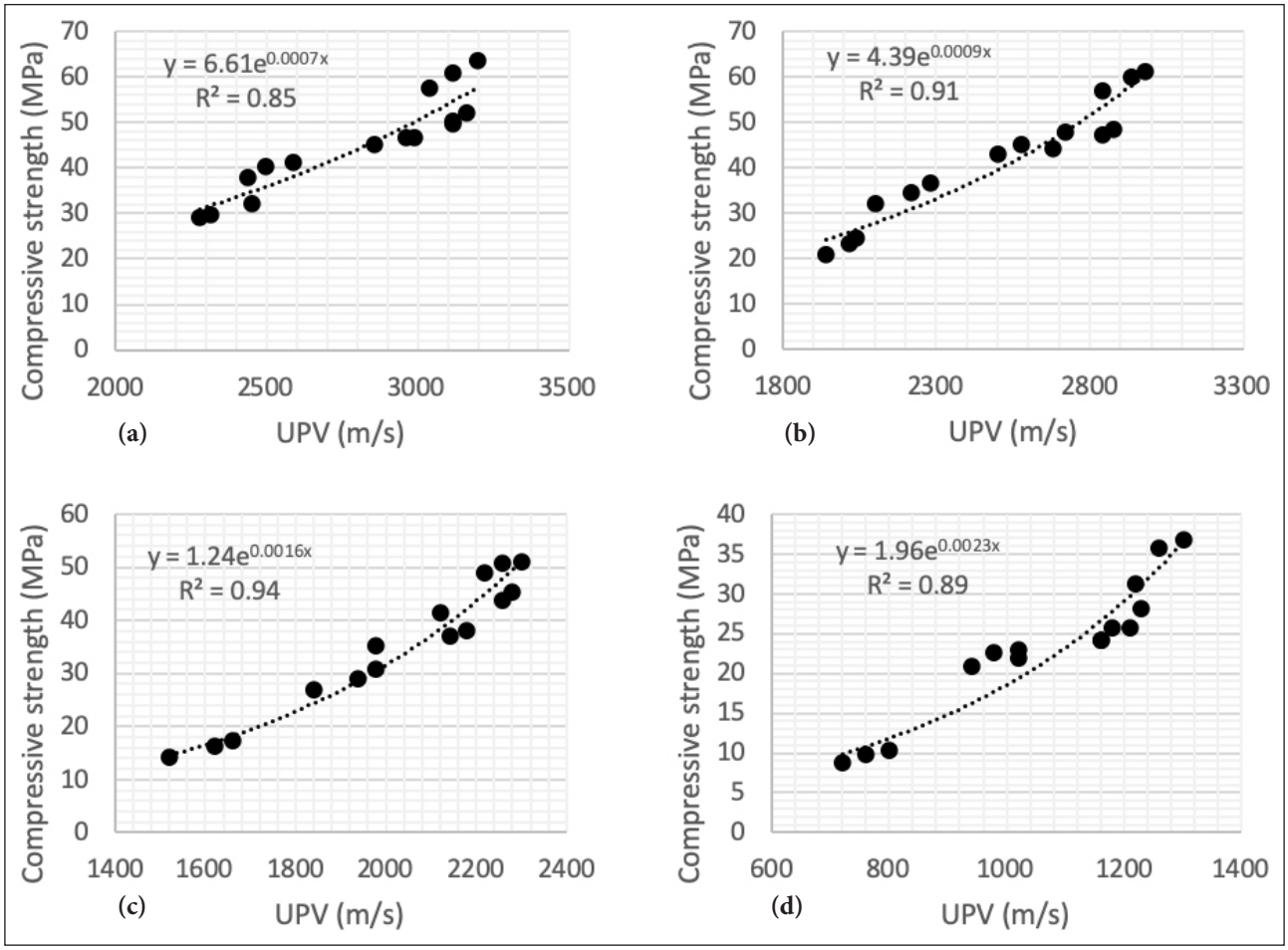

Figure 10. Compressive strength and U.P.V. relationship of samples kept in ambient cured **(a)** before high-temperature **(b)** after 200 °C temperature **(c)** after 400 °C temperature **(d)** after 600 °C temperature.

are shown in Table 5. Except for the TW-10 mixture, decreases in strength were detected at 200 °C for all mixtures cured at 60 °C. At 200 °C, a change in the compressive strength of all mixture series was observed between -5.81% and 1.10%. Similar to 200 °C, the least strength decreases at 400 °C and 600 °C were obtained from mixtures with 10% T.W. replacement. Mixtures using 20% T.W. lost less strength than the control sample, similar to the TW-10 series. The weakest performance at all temperatures was observed in the TW-40 series. In this series, as the temperature increased from 200 to 600 °C, the compressive strength decreased from 5.81% to 66.41%. Heat-cured mixtures gave approximately the same results as mixtures kept in ambient cured. However, the decrease in strength after high temperature in heat-cured samples was less than that in ambient cured.

The reduction in U.P.V. results of specimens cured at 60 °C was between 5.33% and 11.08% at 200 °C. As the temperature increased to 400 °C, there was a significant decrease in U.P.V. values. While the highest decrease was obtained from the control sample with 27.38%, the lowest decrease was calculated in the TW-30 series with 21.80%. At 600 °C, the reduction in U.P.V. values continued and ranged between 49.62% and 63.08%.

In their studies, [54] and [55] obtained a relationship between compressive strength and U.P.V. values based on experimental results using Equation (1) given below.

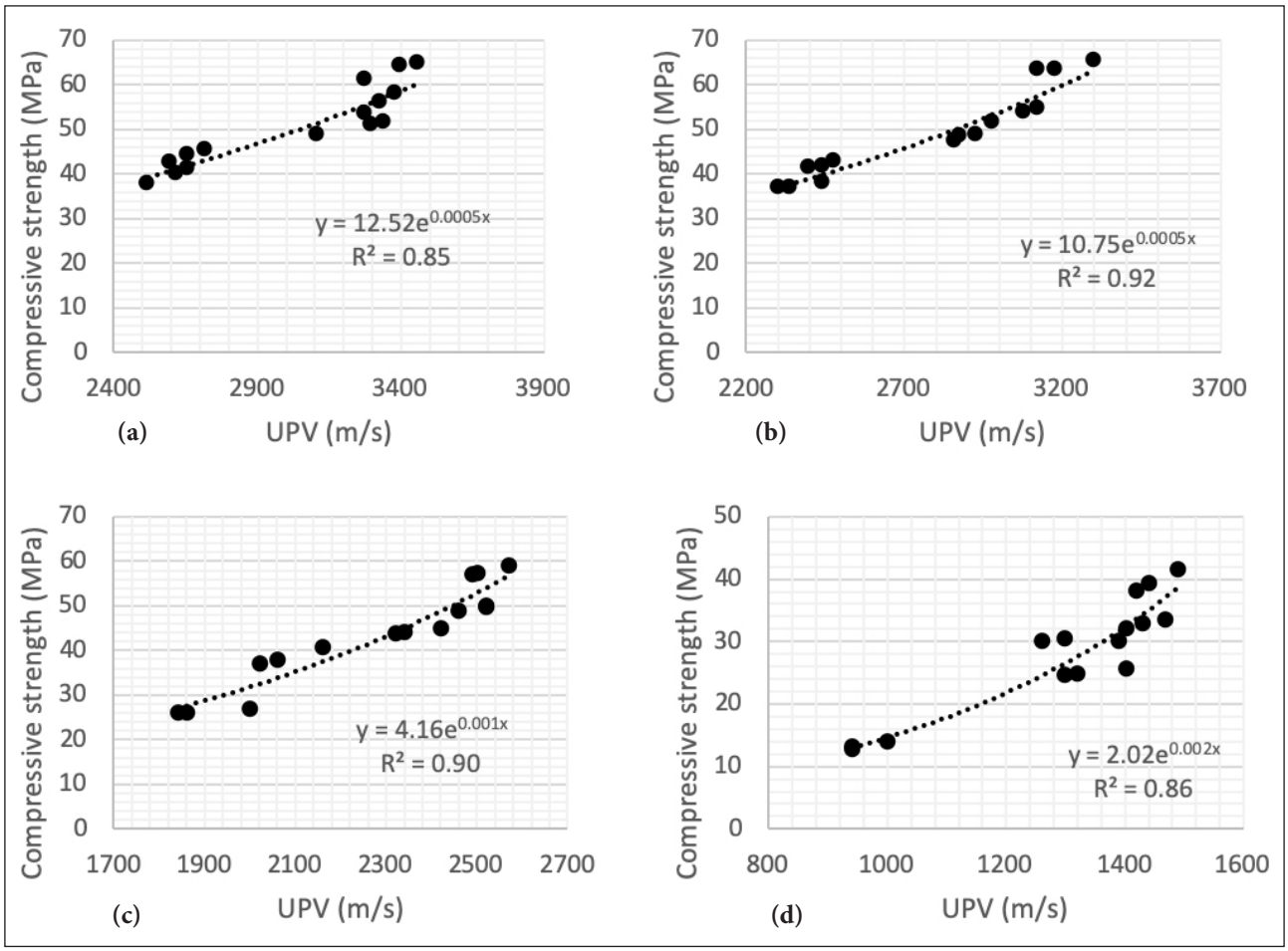

Figure 11. Compressive strength and U.P.V. relationship of samples kept in Heat cured **(a)** before high-temperature **(b)** 200 °C temperature **(c)** 400 °C temperature **(d)** 600 °C temperature.

$f_c = ae^{bV_c}$) (1)

where f_c is the compressive strength, a and b are constants, and Vc is the U.P.V. value.

The relationship between the compressive strength and U.P.V. of the specimens subjected to ambient cured before and after high temperature is given in Figure 10a–d. The relationships between compressive strength and U.P.V. were made using three specimens tested in each mixture. The coefficient of determination (R^2) of the mixture series subjected to ambient cure was approximately 0.87, 0.91, 0.96, and 0.90, respectively. The equations related to the temperature relationship at 23, 200, 400, and 600 °C are given in Equations (2), (3), (4) and (5), respectively.

$f_{c(23\ ^oC)} = 6.61e^{0.0007V_c}$ (2)

$f_{c(200\ ^oC)} = 4.39e^{0.0009V_c}$ (3)

$f_{c(400\ ^oC)} = 1.24e^{0.0016V_c}$ (4)

$f_{c(600\ ^oC)} = 1.96e^{0.0023V_c}$ (5)

The relationship between the compressive strength and U.P.V. of the samples subjected to Heat cured before and after high temperature is presented in Figure 11a–d. The coefficients of determination of heat-cured mixtures at 23, 200, 400, and 600 °C were calculated as 0.87, 0.92, 0.90 and 0.91, respectively. The following equations were determined for 23, 200, 400, and 600 °C, respectively.

$f_{c(23\ ^oC)} = 12.52e^{0.0005V_c}$ (6)

$f_{c(200\ ^oC)} = 10.75e^{0.0005V_c}$ (7)

$f_{c(400\ ^oC)} = 4.16e^{0.001V_c}$ (8)

$f_{c(600\ ^oC)} = 2.02e^{0.002V_c}$ (9)

3.5.1. Mass Loss

The mass loss results of geopolymer mortar mixture samples kept in ambient cured and subjected to high temperatures are given in Figure 12a, and the results of heat-cured samples are shown in Figure 12b. In ambient cure, control sample mass loss ranged from 5.90 to 11.86% in mixtures subjected to ambient cure. The lowest mass loss at 200 °C was obtained from the TW-10 series. The highest mass loss was calculated from thranging, ranging from 9.10% to 13.22%. Significant increases in mass losses occurred after 400 °C. The lowest loss was calculated for all estimated TW-20 series at 7.61%. At 600 °C, the mass loss of all mixtures was more than 10%. At 600 °C, mass loss ranged from 10.64 to 13.22%. The weight loss in geopolymer mortars was due to evaporation of absorption water in the temperature range of 30–210 °C, deterioration of side chains in the temperature range of 210–400 °C, and degradation of leading polymer chains at 400–500 °C. Also, weakening the bond between aggregate and paste at high temperatures increased weight losses [63, 64].

The mass losses of the samples cured at 60 °C decreased compared to those in the ambient cure. The lowest mass

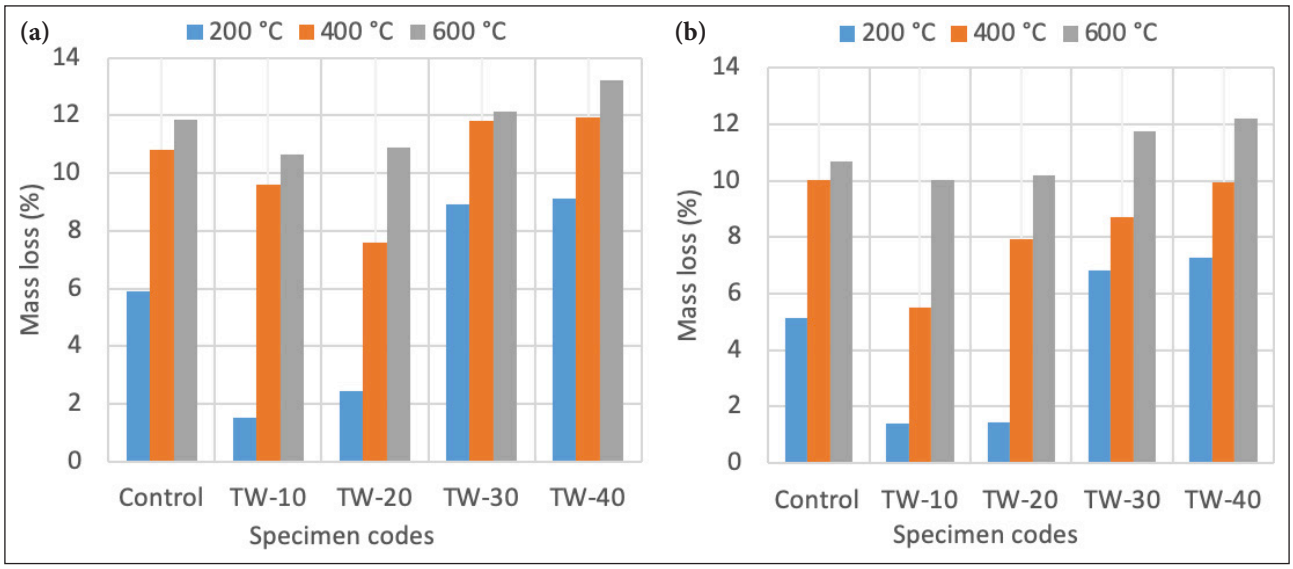

Figure 12. Mass loss of **(a)** ambient and **(b)** 60 °C cured specimens after elevated temperature.

loss at 200 °C was calculated in the TW-10 series at 1.41%. An increase in mass losses was observed with increasing temperature. At 400 °C, mass losses ranged from 5.50% to 12.20%. At 600 °C, as in other temperatures, the lowest mass loss was determined in the TW-10 series.

Within the scope of this study, the use of tincal waste in the production of geopolymer concrete, as an innovative industrial by-product that can be used both to reduce the amount of environmentally harmful waste materials and to replace cement, was examined. Study results show that T.W. is promising in geopolymer concrete production. Future studies should discuss it with different materials, curing temperatures, and alkali silicate activator ratios. In addition, both in this study and in the literature, it is clear that the microstructural properties of the N-A(M)-S-H structure, a vital gel phase especially for high-temperature resistance, require further study.

4. CONCLUSION

In this study, 10%, 20%, 30%, and 40% T.W. was replaced by slag in geopolymer production. The properties of mixtures before and after high temperatures were examined. Information about the results obtained is summarized below.

- The highest 7-day compressive strength in the ambient cured was obtained in the mortar mixture using 10% T.W. An improvement of 30.25% and 7.65%, respectively, was detected in the compressive strength of the mixtures using 10% and 20% T.W. compared to reference mixture.
- The 28th-day strength results of the samples kept in ambient cured vary between 30.30 MPa and 60.70 MPa. The highest pressure values were obtained from the TW-10 series, 28.60% higher than the control sample. Similar to the ambient cured, the highest strength in heat-cured samples was calculated in the TW-10 series.
- The difference in strength between ambient-cured and heat-cured samples at the early ages of cure decreased significantly on the 28th day.
- Using T.W. in samples kept in ambient cure increased the high-temperature resistance. TW-10 and TW-20 series were the mixture series that suffered the least compressive strength loss at 400 °C and 600 °C.
- Except for the TW-10 mixture, decreases in strength were detected at 200 °C for all mixtures at 60 °C. In specimens at 60 °C, the strength losses of TW-10 and control series at 400 °C and 600 °C were determined as 8.68%–37.22% and 12.28%–38.81%, respectively.
- The exponential relationship between compressive strength and U.P.V. before and after exposure to high temperatures, with strong R2 values, reported a sufficient approximation to compare the two.
- Similar to the compressive strength results, the least mass loss was determined in the TW-10 and TW-20 series. The mass loss of heat-cured specimens was less than that of specimens kept in ambient cure.

ETHICS

There are no ethical issues with the publication of this manuscript.

DATA AVAILABILITY STATEMENT

The authors confirm that the data that supports the findings of this study are available within the article. Raw data that support the finding of this study are available from the corresponding author, upon reasonable request.

CONFLICT OF INTEREST

The authors declare that they have no conflict of interest.

FINANCIAL DISCLOSURE

The authors declared that this study has received no financial support.

USE OF AI FOR WRITING ASSISTANCE

Not declared.

PEER-REVIEW

Externally peer-reviewed.

REFERENCES

[1] Schneider, M., Romer, M., Tschudin, M., & Bolio, H. (2011). Sustainable cement production present and future. *Cem Concr Res, 41*, 642–650. [CrossRef]

[2] Benhelal, E., Zahedi, G., Shamsaei, E., & Bahadori, A. (2013). Global strategies and potentials to curb CO2 emissions in cement industry. *J Clean Prod, 51*, 142–161. [CrossRef]

[3] He, Z., Zhu, X., Wang, J., Mu, M., & Wang, Y. (2019). Comparison of CO2 emissions from O.P.C. and recycled cement production. *Constr Build Mater, 211*, 965–973. [CrossRef]

[4] Çelik, Z. (2023). Investigation of the use of ground raw vermiculite as a supplementary cement materials in self-compacting mortars: Comparison with class C fly ash. *J Build Eng, 65*, 105745. [CrossRef]

[5] Gartner, E. (2004). Industrially interesting approaches to "low-CO2" cements. *Cem Concr Res, 34*, 1489–1498. [CrossRef]

[6] Zakka, W. P., Lim, N. H. A. S., & Khun, M. C. (2021). A scientometric review of geopolymer concrete. *J Clean Prod, 280*, 124353. [CrossRef]

[7] Bellum, R. R., Muniraj, K., Indukuri, C. S. R., & Madduru, S. R. C. (2020). Investigation on performance enhancement of fly ash-GGBFS based graphene geopolymer concrete. *J Build Eng, 32*, 101659. [CrossRef]

[8] Prud'homme, E., Michaud, E., Joussein, S., & Rossignol, S. (2012). Influence of raw materials and potassium and silicon concentrations on the formation of a zeolite phase in a geopolymer network during thermal treatment. *J Non-Cryst Solids, 358*, 1908–1916. [CrossRef]

[9] Sahin, F., Uysal, M., Canpolat, O., Cosgun, T., & Dehghanpour, H. (2021). The effect of polyvinyl fibers on metakaolin-based geopolymer mortars with different aggregate filling. *Constr Build Mater, 300*, 124257. [CrossRef]

[10] Mehta, A., & Siddique, R. (2016). An overview of geopolymers derived from industrial by-products. *Constr Build Mater, 127*, 183–198. [CrossRef]

[11] Lin, H., Liu, H., Li, Y., & Kong, X. (2021). Properties and reaction mechanism of phosphoric acid activated metakaolin geopolymer at varied curing temperatures. *Cem Concr Res, 144*, 106425. [CrossRef]

[12] Masi, G., Rickard, W. D. A., Bignozzi, M. C., & Van Riessen, A. (2015). The effect of organic and inorganic fibres on the mechanical and thermal properties of aluminate activated geopolymers. *Compos Part B Eng, 76*, 218–228. [CrossRef]

[13] Wu, Y., Lu, B., Bai, T., Wang, H., Du, F., Zhang, Y., Cai, L., Jiang, C., & Wang, W. (2019). Geopolymer, green alkali activated cementitious material: Synthesis, applications and challenges. *Constr Build Mater, 224*, 930–949. [CrossRef]

[14] Bai, T., Song, Z., Wang, H., Wu, Y., & Huang, W. (2019). Performance evaluation of metakaolin geopolymer modified by different solid wastes. *J Clean Prod, 226*, 114–121. [CrossRef]

[15] Yang, K. H., Song, J. K., & Song, K. I. (2013). Assessment of CO2 reduction of alkali-activated concrete. *J Clean Prod, 39*, 265–272. [CrossRef]

[16] Yang, T., Han, E., Wang, X., & Wu, D. (2017). Surface decoration of polyimide fiber with carbon nanotubes and its application for mechanical enhancement of phosphoric acid-based geopolymers. *Appl Surf Sci, 416*, 200–212. [CrossRef]

[17] Qaidi, S. M. A., Atrushi, D. S., Mohammed, A. S., Ahmed, H. U., Faraj, R. H., Emad, W., Tayeh, B. A., & Najm, H. M. (2022). Ultra-high-performance geopolymer concrete: A review. *Constr Build Mater, 346*, 128495. [CrossRef]

[18] Ismail, I., Bernal, S. A., Provis, J. L., San Nicolas, R., Hamdan, S., & van Deventer, J. S. J. (2014). Modification of phase evolution in alkali-activated blast furnace slag by the incorporation of fly ash. *Cem Concr Compos, 45*, 125–135. [CrossRef]

[19] Gao, X., Yu, Q. L., & Brouwers, H. J. H. (2015). Reaction kinetics, gel character and strength of ambient temperature cured alkali activated slag–fly ash blends. *Constr Build Mater, 80*, 105–115. [CrossRef]

[20] Omur, T., Miyan, N., Kabay, N., Birol, B., & Oktay, D. (2023). Characterization of ferrochrome ash and blast furnace slag based alkali-activated paste and mortar. *Constr Build Mater, 363*, 129805. [CrossRef]

[21] Zhang, H. Y., Qiu, G. H., Kodur, V., & Yuan, Z. S. (2020). Spalling behavior of metakaolin-fly ash based geopolymer concrete under elevated temperature exposure. *Cem Concr Compos, 106*, 103483. [CrossRef]

[22] Mendes, A., Sanjayan, J. G., Gates, W. P., & Collins, F. (2012). The influence of water absorption and porosity on the deterioration of cement paste and concrete exposed to elevated temperatures, as in a fire event. *Cem Concr Compos, 34*, 1067–1074. [CrossRef]

[23] Kuri, J. C., Majhi, S., Sarker, P. K., & Mukherjee, A. (2021). Microstructural and non-destructive investigation of the effect of high temperature exposure on ground ferronickel slag blended fly ash geopolymer mortars. *J Build Eng, 43*, 103099. [CrossRef]

[24] Davidovits, J. (1991). Geopolymers: inorganic polymeric new materials. *J Therm Anal Calorim, 37*, 1633–1656. [CrossRef]

[25] Kong, D. L. Y., & Sanjayan, J. G. (2010). Effect of elevated temperatures on geopolymer paste, mortar and concrete. *Cem Concr Res, 40*, 334–339. [CrossRef]

[26] Lemougna, P. N., Adediran, A., Yliniemi, J., Ismailov, A., Levanen, E., Tanskanen, P., Kinnunen, P., Roning, J., & Illikainen, M. (2020). Thermal stability of one-part metakaolin geopolymer composites containing high volume of spodumene tailings and glass wool. *Cem Concr Compos, 114*, 103792. [CrossRef]

[27] Pan, Z., Tao, Z., Cao, Y. F., Wuhrer, R., & Murphy, T. (2018). Compressive strength and microstructure of alkali-activated fly ash/slag binders at high temperature. *Cem Concr Compos, 86*, 9–18. [CrossRef]

[28] Guerrieri, M., Sanjayan, J., & Collins, F. (2010). Residual strength properties of sodium silicate alkali activated slag paste exposed to elevated temperatures. *Mater Struct, 43*, 765–773. [CrossRef]

[29] Türker, H. T., Balçikanli, M., Durmuş, İ. H., Özbay, E., & Erdemir, M. (2016). Microstructural alteration of alkali activated slag mortars depend on exposed high temperature level. *Constr Build Mater, 104*, 169–180. [CrossRef]

[30] Yang, Z., Mocadlo, R., Zhao, M., Sisson, R.D., Jr., Tao, M., & Liang, J. (2019). Preparation of a geopolymer from red mud slurry and class F fly ash and its behavior at elevated temperatures. *Constr Build Mater, 221*, 308–317. [CrossRef]

[31] Türkmen, İ., Karakoç, M. B., Kantarcı, F., Maraş, M. M., & Demirboğa, R. (2016). Fire resistance of geopolymer concrete produced from Elazığ ferrochrome slag. *Fire Mater, 40*, 836–847. [CrossRef]

[32] Karakoç, M. B., Türkmen, İ., Maraş, M. M., Kantarcı, F., Demirboğa, R., & Toprak, M. U. (2014). Mechanical properties and setting time of ferrochrome slag based geopolymer paste and mortar. *Constr Build Mater, 72*, 283–292. [CrossRef]

[33] Nuaklong, P., Jongvivatsakul, P., Pothisiri, T., Sata, V., & Chindaprasirt, P. (2020). Influence of rice husk ash on mechanical properties and fire resistance of recycled aggregate high-calcium fly ash geopolymer concrete. *J Clean Prod, 252*, 119797. [CrossRef]

[34] Bideci, Ö. S. (2016). The effect of high temperature on lightweight concretes produced with colemanite coated pumice aggregates. *Constr Build Mater, 113*, 631–640. [CrossRef]

[35] Abali, Y., Bayca, S. U., & Targan, S. (2006). Evaluation of blends tincal waste, volcanic tuff, bentonite and fly ash for use as a cement admixture. *J Hazard Mater, 131*, 126–130. [CrossRef]

[36] Turan, E. (2020). *The engineering properties of boron waste clays and its usability in stabilisation of high plasticity clay* [MS thesis, Ataturk University].

[37] Kurt Albayrak, Z.N., & Turan, E. (2019). Kestelek Bor Atık Kili Katkılı Yüksek Plastisiteli Bir Kilin Mukavemet Özelliklerinin Araştırılması. *Iğdır Univ Fen Bil Enst Der, 9*, 890–899. [CrossRef]

[38] Albayrak, Z. N. K., & Turan, E. (2021). The use of boron waste clay to improve the geotechnical properties of a high plasticity clay. *Arab J Geosci, 14*, 1002. [CrossRef]

[39] Kula, I., Olgun, A., Sevinc, V., & Erdogan, Y. (2002). An investigation on the use of tincal ore waste, fly ash, and coal bottom ash as Portland cement replacement materials. *Cem Concr Res, 32*, 227–232. [CrossRef]

[40] Boncukcuoğlu, R., Kocakerim, M. M., Tosunoğlu, V., & Yilmaz, M. T. (2002). Utilization of trommel sieve waste as an additive in Portland cement production. *Cem Concr Res, 32*, 35–39. [CrossRef]

[41] Kürklü, G. (2016). The effect of high temperature on the design of blast furnace slag and coarse fly ash-based geopolymer mortar. *Compos Part B Eng, 92*, 9–18. [CrossRef]

[42] Bouaissi, A., Li, L., Abdullah, M. M. A. B., & Bui, Q. B. (2019). Mechanical properties and microstructure analysis of FA-GGBS-HMNS based geopolymer concrete. *Constr Build Mater, 210*, 198–209. [CrossRef]

[43] Zhang, Z., Zhu, Y., Yang, T., Li, L., Zhu, H., & Wang, H. (2017). Conversion of local industrial wastes into greener cement through geopolymer technology: A case study of high-magnesium nickel slag. *J Clean Prod, 141*, 463–471. [CrossRef]

[44] Haha, M. B., Lothenbach, B., Le Saout, G. L., & Winnefeld, F. (2011). Influence of slag chemistry on the hydration of alkali-activated blast-furnace slag - Part I: Effect of MgO. *Cem Concr Res, 41*, 955–963. [CrossRef]

[45] Uysal, M., Al-mashhadani, M. M., Aygörmez, Y., & Canpolat, O. (2018). Effect of using colemanite waste and silica fume as partial replacement on the performance of metakaolin-based geopolymer mortars. *Constr Build Mater, 176*, 271–282. [CrossRef]

[46] Görhan, G., & Kürklü, G. (2014). The influence of the NaOH solution on the properties of the fly ash-based geopolymer mortar cured at different temperatures. *Compos Part B Eng, 58*, 371–377. [CrossRef]

[47] Shill, S.K., Al-Deen, S., Ashraf, M., & Hutchison, W. (2020). Resistance of fly ash based geopolymer mortar to both chemicals and high thermal cycles simultaneously. *Constr Build Mater, 239*, 117886. [CrossRef]

[48] Al-Majidi, M. H., Lampropoulos, A., Cundy, A., & Meikle, S. (2016). Development of geopolymer mortar under ambient temperature for in situ applications. *Constr Build Mater, 120*, 198–211. [CrossRef]

[49] Criado, M., Palomo, A., & Fernández-Jiménez, A. (2005). Alkali activation of fly ashes. Part 1: Effect of curing conditions on the carbonation of the reaction products. *Fuel, 84*, 2048–2054. [CrossRef]

[50] Swanepoel, J. C., & Strydom, C. A. (2002). Utilisation of fly ash in a geopolymeric material. *Appl Geochem, 17*, 1143–1148. [CrossRef]

[51] Yang, T., Yao, X., Zhang, Z., & Wang, H. (2012). Mechanical property and structure of alkali-activated fly ash and slag blends. *J Sustain Cem Based Mater, 1*, 167–178.

[52] Bobrowski, A., Kmita, A., Starowicz, M., Hutera, B., & Stypuła, B. (2012). Effect of magnesium oxide nanoparticles on water glass structure. *Arch Foundry Eng, 12*(3), 9–12. [CrossRef]

[53] Mihailova, I., Radev, L., Aleksandrova, V., Colova, I., Salvado, I. M. M., & Fernandes, M. H. V. (2015). Carbonate-apatite forming ability of polyphase glass-ceramics in the CaO-MgO-SiO. *J Chem Technol Metall, 50*, 502–511.

[54] Zhang, H. Y., Kodur, V., Wu, B., Cao, L., & Wang, F. (2016). Thermal behavior and mechanical properties of geopolymer mortar after exposure to elevated temperatures. *Constr Build Mater, 109*, 17–24. [CrossRef]

[55] Ali, N., Canpolat, O., Aygörmez, Y., & Al-Mashhadani, M. M. (2020). Evaluation of the 12–24 mm basalt fibers and boron waste on reinforced metakaolin-based geopolymer. *Constr Build Mater, 251*, 118976. [CrossRef]

[56] Aygörmez, Y., Canpolat, O., Al-mashhadani, M. M., & Uysal, M. (2020). A survey on one year strength performance of reinforced geopolymer composites. *Constr Build Mater, 264*, 120267. [CrossRef]

[57] Aygörmez, Y., Canpolat, O., Al-mashhadani, M. M., & Uysal, M. (2020). Elevated temperature, freezing-thawing and wetting-drying effects on polypropylene fiber reinforced metakaolin based geopolymer composites. *Constr Build Mater, 235*, 117502. [CrossRef]

[58] Şahin, F., Uysal, M., Canpolat, O., Aygörmez, Y., Cosgun, T., & Dehghanpour, H. (2021). Effect of basalt fiber on metakaolin-based geopolymer mortars containing rilem, basalt and recycled waste concrete aggregates. *Constr Build Mater, 301*, 124113. [CrossRef]

[59] Jiang, X., Xiao, R., Zhang, M., Hu, W., Bai, Y., & Huang, B. (2020). A laboratory investigation of steel to fly ash-based geopolymer paste bonding behavior after exposure to elevated temperatures. *Constr Build Mater, 254*, 119267. [CrossRef]

[60] Li, C., Sun, H., & Li, L. (2010). A review: The comparison between alkali-activated slag (Si+ Ca) and metakaolin (Si+ Al) cements. *Cem Concr Res, 40*, 1341–1349. [CrossRef]

[61] Lee, N. K., Koh, K. T., An, G. H., & Ryu, G. S. (2017). Influence of binder composition on the gel structure in alkali activated fly ash/slag pastes exposed to elevated temperatures. *Ceram Int, 43*, 2471–2480. [CrossRef]

[62] Yang, T., Wu, Q., Zhu, H., & Zhang, Z. (2017). Geopolymer with improved thermal stability by incorporating high-magnesium nickel slag. *Constr Build Mater, 155*, 475–484. [CrossRef]

[63] He, P., Jia, D., Lin, T., Wang, M., & Zhou, Y. (2010). Effects of high-temperature heat treatment on the mechanical properties of unidirectional carbon fiber reinforced geopolymer composites. *Ceram Int, 36*, 1447–1453. [CrossRef]

[64] Kong, D. L. Y., Sanjayan, J. G., & Sagoe-Crentsil, K. (2007). Comparative performance of geopolymers made with metakaolin and fly ash after exposure to elevated temperatures. *Cem Concr Res, 37*, 1583–1589. [CrossRef]